



Characterization of a new beta titanium alloy, Ti–12Mo–3Nb, for biomedical applications

S.B. Gabriel^{a,b,*}, J.V.P. Panaino^b, I.D. Santos^c, L.S. Araujo^a, P.R. Mei^d, L.H. de Almeida^a, C.A. Nunes^e

^a Universidade Federal do Rio de Janeiro, Departamento de Engenharia Metalúrgica de Materiais, C.P. 68505, Rio de Janeiro (RJ) 21945-970, Brazil

^b Centro Universitário de Volta Redonda, Volta Redonda (RJ), Brazil

^c Pontifícia Universidade Católica do Rio de Janeiro, Rio de Janeiro (RJ), Brazil

^d Universidade Estadual de Campinas, Campinas (SP), Brazil

^e Universidade de São Paulo, Departamento de Engenharia de Materiais, C.P. 116, Lorena (SP) 12.600-970, Brazil

ARTICLE INFO

Article history:

Received 24 October 2011

Accepted 7 November 2011

Available online 6 December 2011

Keywords:

Beta titanium alloy

Niobium addition

Biomedical applications

ABSTRACT

In recent years, different beta titanium alloys have been developed for biomedical applications with a combination of mechanical properties including a low Young's modulus, high strength, fatigue resistance and good ductility with excellent corrosion resistance. From this perspective, a new metastable beta titanium Ti–12Mo–3Nb alloy was developed with the replacement of both vanadium and aluminum from the traditional Ti–6Al–4V alloy. This paper presents the microstructure, mechanical properties and corrosion resistance of the Ti–12Mo–3Nb alloy heat-treated at 950 °C for 1 h. The material was characterized by X-ray diffraction and by scanning electron microscopy. Tensile tests were carried out at room temperature. Corrosion tests were performed using Ringer's solution at 25 °C. The results showed that this alloy could potentially be used for biomedical purposes due to its good mechanical properties and spontaneous passivation.

© 2011 Elsevier B.V. All rights reserved.

1. Introduction

Titanium and its alloys are widely used as orthopedic implants due to their corrosion resistance, biocompatibility, specific strength and lower Young's modulus than other metallic biomaterials such as stainless steel and Co–Cr based alloys [1]. The Ti alloy most widely used in orthopedic applications is the Ti–6Al–4V alloy. Although this alloy presents a lower elastic modulus compared to stainless steel and Co–Cr alloys, studies on this particular alloy have shown that the release of small amounts of V in the human body can induce cytotoxic effects [2].

Recently, a number of studies have focused on the development of metastable beta-type Ti alloys with non-toxic elements such as Mo, Zr, Sn, Ta and Nb [1,3–7] which have advantages over alpha and alpha + beta titanium alloys, including a lower Young's modulus and better toughness [7–9]. Moreover, processing variables can be controlled to produce selected results [10].

Studies carried out by Gordin et al. [7] in the development of a metastable beta-type Ti–12Mo–5Ta (Ti–6.6Mo–1.47Ta %at.) alloy showed that it presented a low Young's modulus (74 GPa)

and high corrosion resistance. Considering the chemical similarity of Nb, as well as its lower cost and lower density (8.56 vs. 16.6 g/cm³) compared to Ta, a new alloy composition was studied, i.e. Ti–12Mo–3Nb. In the design of the chemical composition, the amount of Nb added corresponded in %at. to the replacement of Ta in the Gordin et al. alloy [7]. The focus of the present study was related to the determination of the phase stability, Young's modulus and electrochemical behavior of this novel alloy.

2. Methods

2.1. Material preparation

The Ti–12Mo–3Nb alloy was prepared from commercially pure Ti, Mo and Nb metals by arc melting with a tungsten electrode on a water-cooled copper hearth. The alloy was prepared in a high purity argon atmosphere and the ingot was melted five times to improve chemical homogeneity. The obtained ingot (35 g) was solution-treated at 1000 °C under high vacuum for 24 h inside a tubular furnace, followed by quenching in water at room temperature. It was then swaged at 780–860 °C with an 80% reduction in area. The sample (cylindrical in shape) was solution-treated at 950 °C under high vacuum for 1 h in a tubular furnace, and then quenched in water at room temperature.

2.2. Phase characterization

Phase characterization was carried out using X-ray diffraction (XRD, Shimadzu model XRD 6000 diffractometer) operated at 40 kV, 30 mA and CuK_α radiation ($\lambda = 1.5418 \text{ \AA}$). The phases were identified through comparison with simulated diffractograms using the program Powdercell [11], inserting data of the α , ω and β -Ti phases as space groups, lattice parameters and atomic positions [12].

* Corresponding author at: Universidade Federal do Rio de Janeiro, Departamento de Engenharia Metalúrgica de Materiais, C.P. 68505, Rio de Janeiro (RJ) 21945-970, Brazil. Tel.: +55 2433213848; fax: +55 2122901615.

E-mail address: sinara@metalmat.ufjf.br (S.B. Gabriel).

The microstructure of the alloy was also investigated by scanning electron microscopy (SEM). The sample was ground using silicon carbide papers up to 2400 mesh, polished using standard metallographic techniques and then etched with Kroll's reagent (3 mL HF, 6 mL HNO₃ and 100 mL H₂O).

2.3. Measurement of Young's modulus and tensile tests

The Young's modulus (YM) was determined by the instrumented indentation technique using a Nanoindenter. Three sets of nine indentations were made using a Berkovich tip, with an applied load of 400 mN corresponding to one complete loading–unloading cycle and with a peak hold time of 15 s. The obtained modulus value was the average of 27 measurements. For comparison, the value of the Young's modulus of Ti–6Al–4V was also determined under the same conditions.

Tensile tests were performed at room temperature with specimens with 22.7 mm in length and 4 mm in diameter and using a strain rate of $4 \times 10^{-3} \text{ s}^{-1}$. Two specimens were tested to rupture in the heat-treated condition.

2.4. Electrochemical behavior

The electrochemical behavior was investigated using Ringer's solution. The tests were carried out in a three-electrode corrosion cell; the surface area of the working electrode (Ti–12Mo–3Nb alloy) was 0.206 cm². A platinum wire and an Ag/AgCl electrode (saturated in KCl solution; E° = 0.198 V vs. SHE) were used as the auxiliary and reference electrodes, respectively. The cyclic polarization curves were obtained at 0.5 mV/s.

3. Results and discussion

3.1. Microstructural and mechanical characterization

Fig. 1 shows the XRD pattern of the Ti–12Mo–3Nb alloy treated at 950 °C for 1 h and quenched; only the β phase can be identified in the alloy and the diffraction planes were indexed. The value of the β -stabilizer equivalence (% Mo_{eq}) was calculated as 12.84. This value is higher than 10.0 wt.%, which classifies this alloy in the β -metastable category.

Fig. 2 shows micrographs of the alloy, demonstrating that a single phase could be observed. Thus, the results of the microstructural characterization are identical to those of Gordin et al. [7] and confirm the expected effect of Ta replacement by Nb.

The values obtained for the measurements of Young's modulus using the instrumented indentation technique were 140 GPa for the reference Ti–6Al–4V alloy and 105 GPa for β -Ti–12Mo–3Nb alloy. This indicates a 25% reduction in the Young's modulus of the alloy described in the present work. Considering the data presented by Song et al. [13] by means of electronic structural calculations of binary β -Ti phases, a lower Young's modulus was expected for the β -Ti–12Mo–3Nb (Ti–6.6Mo–1.47Nb %at.) alloy compared to the β -Ti–12Mo–5Ta (Ti–6.6Mo–1.47Ta %at.) alloy. The values of Young's modulus measured by the indentation technique could not be directly compared with data available in the literature obtained using the ultrasonic technique. In the latter case, the values are

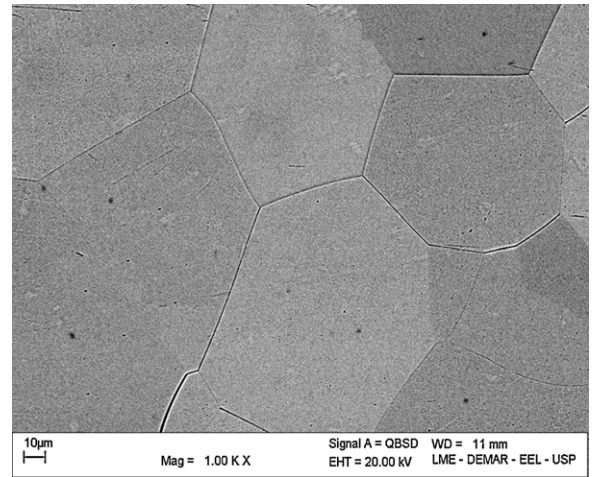


Fig. 2. SEM of the Ti–12Mo–3Nb alloy treated at 950 °C/1 h.

generally lower [14]. In the work of Gordin et al. [7], the ultrasonic technique was used to measure the Ti–12Mo–5Ta alloy as well in the Ti–6Al–4V alloy. The values were 74 GPa and 120 GPa, respectively, which represents a 38% reduction in the Young's modulus.

Fig. 3 shows the stress–strain curve at room temperature of the Ti–12Mo–3Nb alloy. The mean observed values were 747 MPa, 449 MPa and 42% for tensile strength, yield strength and elongation (%), respectively.

In all Ti alloys, the maximization of the ratio of yield strength to Young's modulus should be pursued. A reduction in Young's modulus and an improvement in the strength of the Ti–12Mo–3Nb alloy could be optimized by a suitable aging treatment [15].

Table 1 shows the mechanical properties and the ratio of strength-to-modulus of the Ti–12Mo–3Nb alloy compared with typical biomaterials [16–20]. For load-bearing applications, high strength is important, while a low Young's modulus is desirable to avoid stress shielding. Moreover, an increase in strength is followed by an increase in Young's modulus values [21–23]. As seen in Table 1, the Ti–12Mo–3Nb alloy showed the highest ductility and a higher strength-to-modulus ratio than the Co–Cr–Mo alloys and presented similar values compared to TMZF and Ti–50% Ta (solubilized).

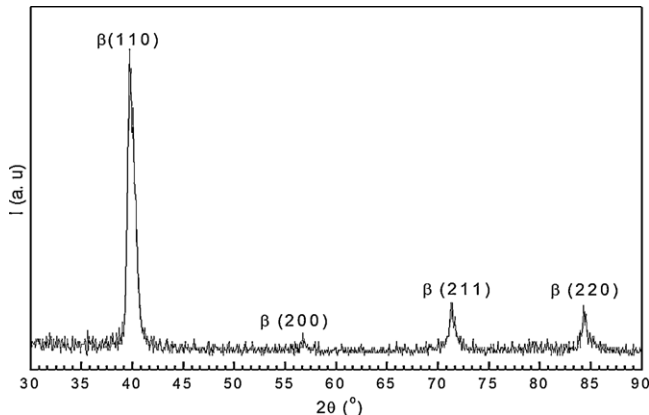


Fig. 1. X-ray diffractogram of the Ti–12Mo–3Nb alloy treated at 950 °C/1 h.

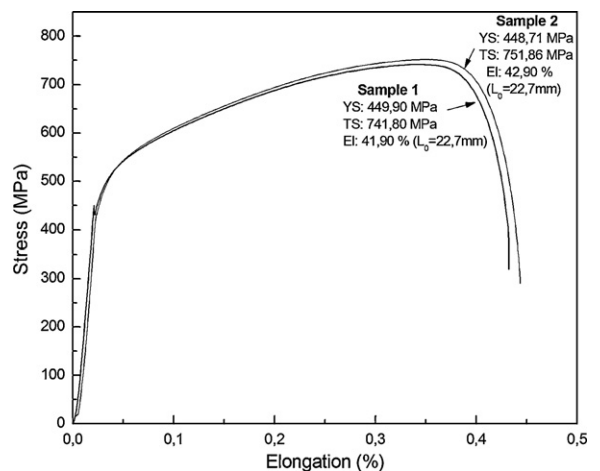


Fig. 3. Stress–strain curves of the Ti–12Mo–3Nb alloy at room temperature.

Table 1
Mechanical properties of typical biomaterials and the Ti–12Mo–3Nb alloy.

Alloy	YM (GPa)	YS (MPa)	Ratio of strength-to-modulus ($\times 10^{-3}$)	EI (%)	Reference
ASTM F75 (Co–Cr–Mo)	220	448	2.0	8	[16]
Ti–6Al–4V	110–140	800–1100	5.7–10	13–16	[17,18]
Ti–50Ta (solubilized)	88	380	4.3	25	[19]
Ti–50Ta (aged)	77/93	612/877	7.9/9.4	11.6/2.6	[19]
TMZF (Ti–12Mo–6Zr–2Fe)	74–85	100–1060	1.2–14.3	18–22	[20]
Ti–15Mo (annealed)	78	544	7.0	21	[20]
Ti–12Mo–3Nb (solubilized)	105	450	4.3	41.2	(this study)

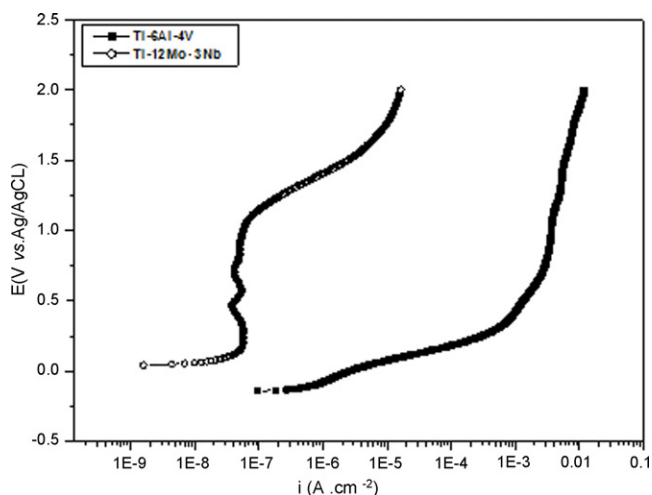


Fig. 4. Potentiodynamic polarization curves of the Ti–12Mo–3Nb and Ti–6Al–4V alloys in Ringer's solution at 25 °C and 0.5 V/min.

3.2. Electrochemical behavior

The electrochemical behavior of Ti–12Mo–3Nb and Ti–6Al–4V alloys in Ringer's solution at 25 °C is presented in Fig. 4; both alloys exhibited spontaneous passivation. It can be observed that the polarization curves of the alloys are different. For the Ti–12Mo–3Nb alloy, the corrosion potential was obtained at about 45 mV (Ag/AgCl) while for the Ti–6Al–4V alloy this was found at about –140 mV (Ag/AgCl), indicating that the passive film which formed on the surface of the Ti–12Mo–3Nb alloy was less stable than the film which formed on the surface of the Ti–6Al–4V alloy. It can also be observed in Fig. 4 that for the Ti–12Mo–3Nb alloy, the passivation region was reached at higher values of current density when compared to the Ti–6Al–4V alloy.

The lower corrosion resistance of the Ti–12Mo–3Nb alloy compared to the Ti–6Al–4V alloy can be attributed to the different chemical composition and microstructure of the oxides which formed on the material's surface. Gordin et al. [7] studied the electrochemical behavior of a beta Ti–12Mo–5Ta alloy in Ringer's solution and observed that Ti–Mo–Ta alloy presented similar behavior to a Ti–Al–V alloy. According to Zhou et al. [1], the corrosion resistance of Ti–Ta alloys improves with an increase in the tantalum concentration due to the good stability of the passive film of Ta₂O₅ which forms on the material's surface. In this way, the behavior observed with the alloy studied in this work (Ti–12Mo–3Nb), with lower corrosion resistance compared to the Ti–12Mo–5Ta alloy, can be attributed to the lower stability of niobium oxides formed in relation to tantalum oxides present in alloys containing tantalum [1,7].

4. Conclusions

The results show that the Ti–12Mo–3Nb alloy could potentially be used for biomedical proposes. It showed excellent ductility and good mechanical properties including a low elastic modulus in the solution-treated condition.

This alloy exhibited spontaneous passivation, although the corrosion potential obtained for the Ti–12Mo–3Nb alloy was at about 45 mV (Ag/AgCl), while for Ti–6Al–4V this value was at about –140 mV (Ag/AgCl), indicating that the passive film which formed on the surface of the Ti–12Mo–3Nb alloy was less stable than the film which formed on the surface of the Ti–6Al–4V alloy.

Acknowledgements

This work was supported by CNPq, FAPERJ and CAPES.

References

- [1] Y.L. Zhou, M. Niinomi, T. Akahori, H. Fukui, H. Toda, Mater. Sci. Eng. A 398 (2005) 28–36.
- [2] D. Kuroda, M. Niinomi, M. Morinaga, et al., Mater. Sci. Eng. A 243 (1998) 244–249.
- [3] S.B. Gabriel, C.A. Nunes, G.A. Soares, Artif. Organs 32 (2008) 299–304.
- [4] S.B. Gabriel, J. Dille, C.A. Nunes, G.A. Soares, Mater. Res. 13 (2010) 1–5.
- [5] A. Cremasco, W.H. Osório, C.M.A. Freire, A. Garcia, R. Caram, Electrochim. Acta 53 (2008) 4867–4874.
- [6] C.R.M. Afonso, G.T. Aleixo, A.J. Ramirez, R. Caram, Mater. Sci. Eng. C 27 (2007) 908–913.
- [7] D.M. Gordin, T. Gloriant, Gh. Nemtoi, R. Chelariu, N. Aelenei, A. Guillou, D. Ansel, Mater. Lett. 59 (2005) 2959–2964.
- [8] R. Banerjee, S. Nag, H.L. Fraser, Mater. Sci. Eng. C 25 (2005) 282–289.
- [9] W. Xu, K.B. Kim, J. Das, et al., Scripta Mater. 54 (2006) 1943–1948.
- [10] N.T.C. Oliveira, G. Aleixo, R. Caram, A.C. Guastaldi, Mater. Sci. Eng. A 452–453 (2007) 727–731.
- [11] W. Kraus, G.J. Nolze, Powdercell – A program for the representation and manipulation of crystal structure and calculation of the resulting X-ray powder patterns, J. Appl. Crystallogr. 29 (1996) 301–303.
- [12] P. Villars, L.D. Calvert, Pearson's Handbook of Crystallographic Data for Intermetallic Phases, second ed., Metals Park, Ohio, 1991.
- [13] Y. Song, D.S. Xu, R. Yang, D. Li, W.T. Wu, Z.X. Guo, Mater. Sci. Eng. A 260 (1999) 269–274.
- [14] S.B. Gabriel, A. Mikowski, P. Soares, C.M. Lepienski, N.K. Kuromoto, C.A. Nunes, G.A. Soares, 6th Brazilian Materials Research Society Meeting, Brazil, 2007.
- [15] Y.L. Zhou, M. Niinomi, T. Akahori, H. Fukui, H. Toda, Mater. Sci. Eng. A 384 (2004) 92–101.
- [16] M. Hunt, Mater. Eng. 113 (1991) 27–31.
- [17] H. Matsumoto, S. Watanabe, S. Hanada, Mater. Sci. Eng. A 448 (2007) 39–48.
- [18] C. Leyens, M. Peters (Eds.), Titanium and Titanium Alloys Fundamentals and Applications, Wiley-VCH GmbH & Co. KGaA, 2003, pp. 20–21.
- [19] Y. Zhou, M. Niinomi, J. Alloys Compd. 466 (2008) 535–542.
- [20] M. Niinomi, Mater. Sci. Eng. A 243 (1998) 231–236.
- [21] P.J. Bania, G.A. Lenning, J.A. Ball, in: R.R. Boyer, H.W. Rosenberg (Eds.), Beta Titanium Alloys in the 1980, AIME, Warrendale, PA, 1984, pp. 209–229.
- [22] P. Ganesan, R.J. Deanglis, G.A. Sargent, J. Less-Comm. Met. 34 (1974) 209.
- [23] Y.T. Lee, G. Welsch, Mater. Sci. Eng. A 128 (1990) 77.